

# Carbamazepine Kinetic Model Solved by a New Flow Graph Method

LAURIAN VLASE<sup>1,\*</sup>, MARIUS SOCOL<sup>2</sup>, ANCA CIURTE<sup>3</sup>, DANA MUNTEAN<sup>1</sup>, IOAN BALDEA<sup>2</sup>, SORIN E. LEUCUTA<sup>1</sup>

<sup>1</sup> University of Medicine and Pharmacy "Iuliu Hatieganu", Faculty of Pharmacy, Department of Pharmaceutical Technology and Biopharmaceutics, 13 Emil Isac, 400023, Cluj-Napoca, Romania

<sup>2</sup> "Babeş-Bolyai" University, Faculty of Chemistry and Chemical Engineering, Department of Physical Chemistry, 11 Arany Janos, 400028, Cluj-Napoca, Romania

<sup>3</sup> "Babeş-Bolyai" University, Department of Informatics, 1 Kogalniceanu, 400048, Cluj-Napoca, Romania

*We have proposed an alternative method based on flow graph principles for solving the linear homogenous differential equation systems with constant coefficients used in kinetic analysis, no matter the number of the unknowns is. The classical method for solving these systems using flow graphs entails Laplace transforms before depicting a flow graph and the reverse transformation after using the Mason's rules for calculus. Our method avoids the complicated calculus using Laplace transforms simplifying the graphing algorithm and permits to find the analytical solutions directly by inspecting the pharmaco-kinetic mechanism. Both methods provide the analytical solutions, eliminating the error propagation occurring in the numerical analysis. The numerical analysis and the alternative flow graph method were applied to a pharmacokinetic model (involving parent drug and metabolite kinetics, pre- and systemic metabolism, distribution) and the corresponding pharmaco-kinetic parameters have been compared.*

*Keywords: flow graph, pharmacokinetics, carbamazepine, differential equation system*

In the kinetic-pharmacokinetic (PK) analysis, there are frequent cases in which the drug absorption and disposition are quite complex and therefore cannot be characterized by classical pharmacokinetic models. For instance, the case of monitoring the drug and its metabolite is a complex one due to the involved presystemic metabolism forming active substances, and due to the complicated distribution processes [1-3].

In that case one has to write a linear system of differential equations describing each kinetic process and to use them for finding the corresponding pharmacokinetic parameters.

The differential equations are easy to write and implement in specialized software, this being the main advantage of the numerical analysis procedure. However, this technique has also some limitations. Numerical solutions are always approximations, and this may cause errors, e.g. in the estimation of derivatives (as required for many fitting algorithms). Another disadvantage of using differential equations is that the convergence toward the estimation solution is rather slower as compared to the case of using the analytical solution [4,5]. This aspect may be important when one deals with large amount of data, especially in population PK analysis.

Analytical solutions provide the calculation of pharmacokinetic parameters with more accuracy, which is indeed an advantage. The analytical solutions could be obtained for linear differential equations systems by using the classical integration [6], the operator method, secular equation and eigenvalues method, constant variation method [7,8] and flow graph method [9-13].

For the first time, by means of a flow graph method, the analytical solution can be obtained directly by inspection the graphical representation of the pharmacokinetic model. However, this method is limited only to the linear homogeneous and non-homogeneous differential equation complex systems but with reduced dimensions or to the

systems with non-limited unknowns number but with low complexity (e.g. consecutive reactions).

## Experimental part

### Kinetic data and model

In order to verify and compare the two methods of data analysis, namely numerical integration and our method using flow graphs, real pharmacokinetic data were used. The data were collected from a bioequivalence study of carbamazepine (CBZ), when both parent drug and its active metabolite (10,11-epoxy-carbamazepine, ECBZ) were determined from time to time.

To describe the absorption and disposition of CBZ and ECBZ, a pharmacokinetic model has been considered (fig. 1). This model involves a first-order kinetic process for absorption of CBZ and bicompartamental distribution. CBZ can be transformed into ECBZ by both presystemic and systemic metabolism. CBZ and ECBZ can be also eliminated from the human body by either metabolic or non-metabolic paths. As the intravenous data for CBZ and ECBZ were not available, the distribution volume for both drugs was considered equal. A lag time for absorption was also considered (Tlag).

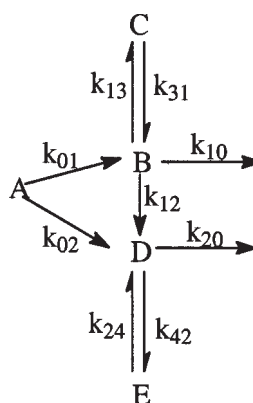


Fig. 1 Kinetic model for carbamazepine and 10,11-epoxy-carbamazepine

\* email: vlaselaur@yahoo.com

The significance of the notations in figure 1 is as follows: *A* stands CBZ at administration place, *B* stands for CBZ in central compartment, *C* for CBZ in peripheral compartment, *D* for ECBZ in central compartment and *E* for ECBZ in peripheral compartment; the rate coefficients are:  $k_{01}$  - absorption rate constant for CBZ,  $k_{02}$  and  $k_{12}$  presystemic and systemic metabolism rate constant of CBZ to ECBZ,  $k_{13}$  and  $k_{31}$  the distribution rate constants for CBZ,  $k_{10}$  and  $k_{20}$  the elimination rate constants for CBZ and ECBZ,  $k_{24}$  and  $k_{42}$  are the distribution rate constants for ECBZ. The initial dose of administered CBZ is denoted by  $X_0$  (the amount of *A* at time=0, e.g. 400 mg CBZ).

The corresponding differential equations for the kinetic model for CBZ and ECBZ (fig.1) are shown in figure 2. The differential equations are using the amounts of *A-E* species, however, in practice one can measure only the concentrations of *B* and *D* (CBZ and ECBZ in plasma – central compartment). Thus, in order to fit the experimental data using the kinetic model, one need a scaling factor between amount and concentration of the measured species, this being the volume of distribution (*Vd*). Both *B* and *D* species are determined in the same place (human plasma), so they have the same *Vd* value. Another model parameter to be estimated by the model is the lag-time for absorption (*Tlag*). In pharmaco-kinetic experiments the time measurement starts at the moment of drug administration. However, the absorption process is usually delayed to the administration time (*Tlag*), as the administered pharmaceutical form have to be first disintegrated in the gastrointestinal tract and the drug have to be released and dissolved in the local liquid media, the absorption begins only after these processes. The *Tlag* parameter is not directly coded in the differential equations of the kinetic model, however, depending on *Tlag* values in comparison with the variable “time”, the model uses a certain set of equations. If the time is less than *Tlag*, there is no kinetic process and all the differential equations are 0. When time reaches *Tlag* all the kinetic processes are started and the second set of equations is used. Like the *Vd*, *Tlag* is also a model parameter to be estimated.

All the pharmacokinetic calculations (using either differential or analytical equations) were made using WinNonlin software (Pharsight, Mountain View, CA, USA).

#### Analysis using the alternative flow graphs method General presentation of flow graph method

A flow graph is a diagram derived from a set of simultaneous linear algebraic equations or a linear differential equations system, which are written (in this case) starting from a set of elementary chemical reactions

on mass transfer included into a mechanism. The flow graph is used to represent the evolution of a physical system and to obtain the relationships between the system variables.

A flow graph consists of a network in which nodes (or vertices) are connected by directed *edges* (or branches). Each node represents a mechanism species, and each edge connecting two nodes acts as a signal multiplier. This multiplication factor, named *transmittance*, can be obtained from the mechanism kinetic constants. An arrow placed on the edge indicates the direction of the signal flow and the multiplication factor is indicated along the edge [14,15]. The signal flow graph depicts the flow of signals from one point of the graph to another (a path or a way) and gives the relationships between the signals [9]; a path should not go out any node of the graph more than once (only one outgoing edge) and every inner node of the graph has to be touched. A forward path is a path starting from an input node (or source, a node which has only the outgoing edges) or from one - continue path - or more - discontinue path - mixed nodes (a node which has incoming and outgoing edges) to one or more output nodes (a node which has only the incoming edges) [9,15]. The product of the transmittances of a forward path is named the gain of the path (FWG). The gain of the flow graph is the sum of the all forward path gains [9-13].

In the case of solving a linear differential equations system, we associate for every determinant of the system a flow graph. The value of determinant is the gain of the associated flow graph. The flow graph associated with the secular determinant [15] is named the consumption flow graph and is derived directly from mechanistic model; based on the gain of the consumption flow graph, one obtains the eigenvalues ( $\gamma_i$ ) and the consumption determinants ( $\Delta_c$ ) which represent the products of differences of the eigenvalues. The flow graphs associated with the determinants obtained by replacing the columns of the secular determinant with the column of free coefficients (the formation determinants), are named the formation flow graphs [16] and they are depicted for every species starting from the consumption flow graph.

The general mathematical solutions of the linear differential equations systems are the sum of exponential functions [6-9] (e.g.  $C_B = B_1 \cdot \exp(-\gamma_1 t) + B_2 \cdot \exp(-\gamma_2 t) + B_3 \cdot \exp(-\gamma_3 t)$ ). In our approach, the pre-exponential coefficients (in this example,  $B_i$ ) represent the ratio of the corresponding formation and consumption determinants, (in accordance with Cramer's rule [17]).

This new graphical method has not required writing the equations system but only the pharmacokinetics model.

$$\begin{array}{l}
 \text{Eq1} \left\{ \begin{array}{l}
 \text{If time} < T_{lag} : \\
 \frac{\partial A}{\partial t} = 0 \\
 \frac{\partial B}{\partial t} = 0 \\
 \frac{\partial C}{\partial t} = 0 \\
 \frac{\partial D}{\partial t} = 0 \\
 \frac{\partial E}{\partial t} = 0 \\
 C_B = 0 \\
 C_D = 0
 \end{array} \right. \\
 \text{Eq2} \left\{ \begin{array}{l}
 \text{If time} \geq T_{lag} : \\
 \frac{\partial A}{\partial t} = -k_{01} \cdot A - k_{02} \cdot A \\
 \frac{\partial B}{\partial t} = k_{01} \cdot A + k_{31} \cdot C - k_{13} \cdot B - k_{10} \cdot B - k_{12} \cdot B \\
 \frac{\partial C}{\partial t} = k_{13} \cdot B - k_{31} \cdot C \\
 \frac{\partial D}{\partial t} = k_{02} \cdot A + k_{12} \cdot B + k_{24} \cdot E - k_{42} \cdot D - k_{20} \cdot D \\
 \frac{\partial E}{\partial t} = k_{42} \cdot D - k_{24} \cdot E \\
 C_B = \frac{B}{Vd} \\
 C_D = \frac{D}{Vd}
 \end{array} \right.
 \end{array}$$

Fig. 2 The differential equations corresponding to the kinetic model for carbamazepine and 10,11-epoxy-carbamazepine. Eq1 is used when time < *Tlag*, Eq2 is used when time ≥ *Tlag*

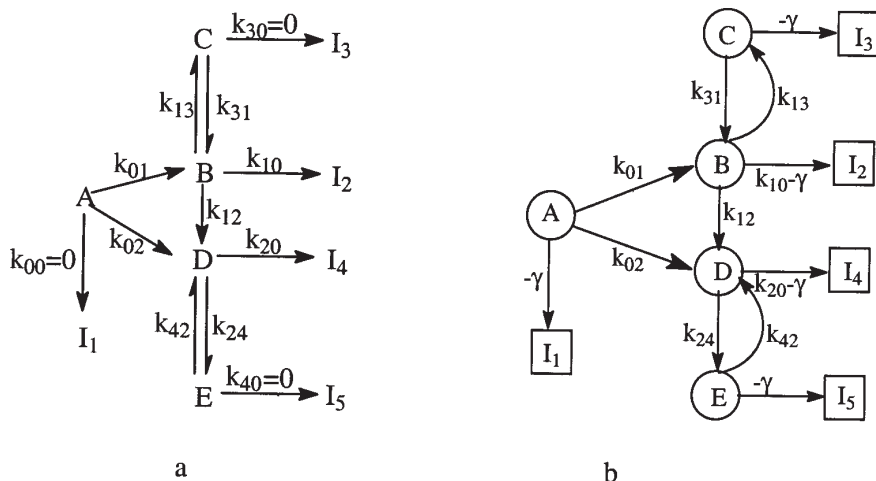


Fig. 3. The equivalent mechanism (a) and consumption flow graph (b)

Solving the kinetic model by using the new graphical method

In this approach a new mechanism equivalent to the model from figure 1 is drawn considering that every substance is transforming in a final product with a constant rate, even it is zero (fig. 3a). The consumption flow graph [16] is the image of the new mechanism with the  $\gamma$  decreased from every output transmittance (fig. 3b). Its name suggests that the system evolution bring about a loss (consumption) in all variable values and a gain of the output values (the final products  $I_1, I_2, I_3$  and  $I_4$ ) in how the arrows indicate the direction of the flux from all mixed nodes to the output nodes.

The formation flow graph [16] for a species is constructed considering the species of interest as being a target one (the final product, an output node) and adding a new node (the input node or the source which represents the initial conditions). They are named like this because indicate a formation and a gain of the chosen variable starting from an input node (the source  $S$ ).

One has identified all forward paths [18] (FW, fig. 3b) and by adding its gains (FWG, e.g.  $FWG1 = k_{01}k_{12}(k_{20}-\gamma)k_{31}k_{42}$ ), one obtains the gain of the consumption flow graph (CG), which, according to the definition, is equal with the value of the secular determinant [19],  $\Delta$ :

$$\Delta = CG = \sum FWGi = (k_{01} + k_{02} - \gamma) \cdot [(-\gamma)(k_{12} + k_{10} - \gamma) + k_{13}(-\gamma) + k_{31}(k_{12} + k_{10} - \gamma)] \cdot [(-\gamma)(k_{20} - \gamma) + k_{42}(k_{20} - \gamma) + k_{24}(-\gamma)] = 0 \quad (1)$$

$$\Delta = (k_{01} + k_{02} - \gamma)[\gamma^2 - \gamma(k_{12} + k_{13} + k_{10} + k_{31}) + k_{31}(k_{12} + k_{10})][\gamma^2 - \gamma(k_{20} + k_{24} + k_{42}) + k_{20}k_{42}] = 0$$

From the above equation it can be found the exponential factors and the expressions of consumption determinants ( $\Delta_c$ ):

$\gamma_1 = k_{01} + k_{02}$ ,  $\gamma_2, \gamma_3$  (the solutions of the first square equation from the last product of  $\Delta$ ), and  $\gamma_4, \gamma_5$  (the solutions of the second square equation from the last product of  $\Delta$ ). Also,

$$\Delta_c(\gamma_i) = \prod_{\substack{j=1 \\ i \neq j}}^n (\gamma_j - \gamma_i), \quad (2)$$

where  $n$  is number of inner nodes.

The formation flow graph for B (fig. 4) is depicted from the consumption flow graph, considering the species of interest being a target one (a final product); the output edges of B species are rejected and a new input node is added (source  $S$  which represents the initial conditions). From the figure 3b, it is clear that no any connections emerge from the node D to the node B, thus the D species will not appear in the formation flow graph of B species.

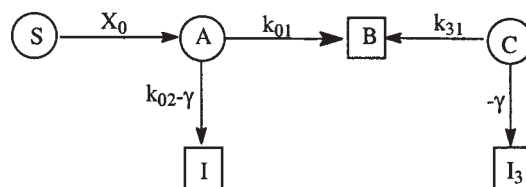


Fig. 4. The formation flow graph for B species

Now node I denotes the output node of A species whose transmittance is the sum of all its outgoing edge transmittances when the node D is missing.

To calculate the gain of the above formation graph one has to choose only the forward paths, which connect the input node with the target species B [9-13] (e.g. the discontinue forward path  $X_0(k_{02}-\gamma)k_{31}$  does not directly link the node  $S$  with B species). The formation determinant is then:

$$\Delta_{Bi} = X_0 \cdot k_{01} \cdot k_{31} + X_0 \cdot k_{01} \cdot (-\gamma_i) = X_0 \cdot k_{01} \cdot (k_{31} - \gamma_i) \quad i = 1, 2, 3; \quad (3)$$

The final solution is presented below:

$$C_B = \frac{X_0 k_{01} (k_{31} - \gamma_1) e^{-\gamma_1 t}}{(\gamma_2 - \gamma_1)(\gamma_3 - \gamma_1)} + \frac{X_0 k_{01} (k_{31} - \gamma_2) e^{-\gamma_2 t}}{(\gamma_1 - \gamma_2)(\gamma_3 - \gamma_2)} + \frac{X_0 k_{01} (k_{31} - \gamma_3) e^{-\gamma_3 t}}{(\gamma_1 - \gamma_3)(\gamma_2 - \gamma_3)} \quad (4)$$

The formation flow graph for D is:

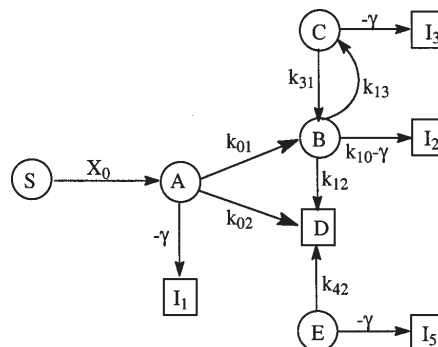


Fig. 5. The formation flow graph for D species

The formation determinants and the solution for  $D$  species are:

$$\Delta_{D_i} = X_0 \cdot k_{01} \cdot k_{12} \cdot (k_{31} - \gamma_i)(k_{42} - \gamma_i) + X_0 \cdot k_{02} \cdot (k_{42} - \gamma_i) \cdot [(k_{31} - \gamma_i)(k_{10} + k_{12} - \gamma_i) + k_{13} \cdot (-\gamma)]$$

$$= X_0 \cdot k_{01} \cdot k_{12} \cdot (k_{31} - \gamma_i) \cdot (k_{42} - \gamma_i) + X_0 \cdot k_{02} \cdot (k_{42} - \gamma_i) \cdot [\gamma_i^2 - \gamma_i(k_{10} + k_{12} + k_{13} + k_{31}) + k_{31} \cdot (k_{10} + k_{12})]$$

$i=1,2,3,4;$

$$C_D = \frac{X_0 \cdot (k_{01} \cdot k_{12} \cdot (k_{31} - \gamma_1) \cdot (k_{42} - \gamma_1) + k_{02} \cdot (k_{42} - \gamma_1) \cdot [\gamma_1^2 - \gamma_1(k_{10} + k_{12} + k_{13} + k_{31}) + k_{31} \cdot (k_{10} + k_{12})]) \cdot e^{-\gamma_1 t}}{(\gamma_2 - \gamma_1)(\gamma_3 - \gamma_1)(\gamma_4 - \gamma_1)(\gamma_5 - \gamma_1)} +$$

$$\frac{X_0 \cdot k_{01} \cdot k_{12} \cdot (k_{31} - \gamma_2) \cdot (k_{42} - \gamma_2) \cdot e^{-\gamma_2 t}}{(\gamma_1 - \gamma_2)(\gamma_3 - \gamma_2)(\gamma_4 - \gamma_2)(\gamma_5 - \gamma_2)} + \frac{X_0 \cdot k_{01} \cdot k_{12} \cdot (k_{31} - \gamma_3) \cdot (k_{42} - \gamma_3) \cdot e^{-\gamma_3 t}}{(\gamma_1 - \gamma_3)(\gamma_2 - \gamma_3)(\gamma_4 - \gamma_3)(\gamma_5 - \gamma_3)} +$$

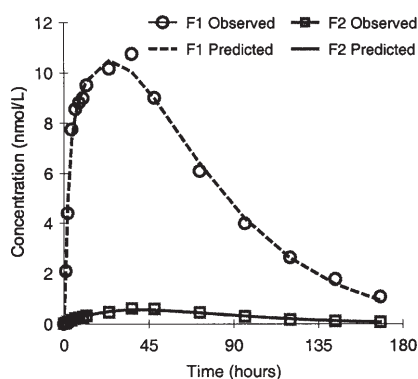
$$\frac{X_0 \cdot (k_{01} \cdot k_{12} \cdot (k_{31} - \gamma_4) \cdot (k_{42} - \gamma_4) + k_{02} \cdot (k_{42} - \gamma_4) \cdot [\gamma_4^2 - \gamma_4(k_{10} + k_{12} + k_{13} + k_{31}) + k_{31} \cdot (k_{10} + k_{12})]) \cdot e^{-\gamma_4 t}}{(\gamma_1 - \gamma_4)(\gamma_2 - \gamma_4)(\gamma_3 - \gamma_4)(\gamma_5 - \gamma_4)} +$$

$$\frac{X_0 \cdot (k_{01} \cdot k_{12} \cdot (k_{31} - \gamma_5) \cdot (k_{42} - \gamma_5) + k_{02} \cdot (k_{42} - \gamma_5) \cdot [\gamma_5^2 - \gamma_5(k_{10} + k_{12} + k_{13} + k_{31}) + k_{31} \cdot (k_{10} + k_{12})]) \cdot e^{-\gamma_5 t}}{(\gamma_1 - \gamma_5)(\gamma_2 - \gamma_5)(\gamma_3 - \gamma_5)(\gamma_4 - \gamma_5)}$$

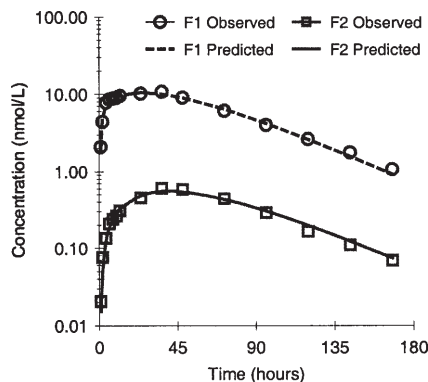
A computer program was executed in the Java language. It recognizes all the forward paths and calculates the gains of the consumption and formation flow graphs [20]. Generally, if the polynomial degrees of the factors from the product of  $\Delta$  in equation (1) is inferior or equal with 4 one can find the symbolic expressions of the eigenvalues ( $\gamma_i$ ), but if it is superior to 4 the numerical solutions of eigenvalues are calculated in the same time with the fitting of the real experimental data.

## Results and discussions

Equation (4) and respectively equation (6) represent the analytical solutions for CBZ (B) and ECBZ (D) in central compartment. A fitting plot of data using the considered pharmacokinetic model is presented in figure 6 (analytical solutions used). It can be noticed that the agreement with the experimental data is very good.



a)



b)

Fig. 5 Fitting plot of kinetic model to the data: (a) the overall view and (b) logarithmic scale; F1-CBZ, F2-ECBZ

Table 1

COMPARISON BETWEEN KINETIC PARAMETERS OF CBZ AND ECBZ OBTAINED BY USING NUMERICAL INTEGRATION METHOD AND ANALYTICAL SOLUTIONS AND STATISTICAL DATA REGARDING PARAMETER ESTIMATION AND MODEL DIAGNOSTICS

Parameter	Unit	Numerical solutions			Analytical solutions			Difference between estimates (%)
		Value	Standard Error	CV%	Value	Standard Error	CV%	
$k_{10}$	$h^{-1}$	0.195368	0.152337	78.79	0.195	0.152131	78.02	-0.16
$k_{20}$	$h^{-1}$	0.240881	0.332125	132.77	0.245881	0.314893	128.07	2.1
$k_{12}$	$h^{-1}$	0.013134	0.014161	101.43	0.013134	0.013915	105.95	0
$k_{13}$	$h^{-1}$	0.422876	0.121555	28.91	0.423	0.111382	26.33	0.3
$k_{31}$	$h^{-1}$	0.107113	0.021891	20.49	0.107	0.020134	18.82	-0.1
$k_{01}$	$h^{-1}$	0.025387	0.017670	69.35	0.025387	0.016654	65.6	0
$k_{02}$	$h^{-1}$	$1.43 \cdot 10^{-4}$	0.000494	474.81	$1.78 \cdot 10^{-4}$	0.00035	196.63	24.5
$k_{24}$	$h^{-1}$	0.788298	0.960750	123.44	0.907298	0.952438	104.98	15
$k_{42}$	$h^{-1}$	0.349274	1.326444	368.28	0.375274	1.314581	350.3	7.4
Volume	L	4218.811	1240.08	29.19	4218.811	1220.32	28.93	0
$T_{lag}$	h	0.559831	0.117656	21.09	0.56043	0.108542	19.38	0.11

### Model diagnostics

SSR*	1.4123	1.121
Corr**	0.9911	0.9923
AIC***	32.357	32.352

\* sum of squares of residuals; \*\* correlation observed-predicted data;

\*\*\* Akaike information criteria=  $2 \cdot (\text{no. of parameters}) + (\text{no. of experiments}) \cdot \ln(\text{SSR})$ ;

CV%= coefficient of variation from mean

The values of kinetic parameters of CBZ and ECBZ (for one set of data), their estimation precision and model diagnostics data, obtained using numerical integration method and analytical equations are presented in table 1.

The analysis of correlation matrix between model parameters did not show any highly correlated parameters (data not shown).

Examining the values obtained for calculated kinetic parameters in table 1, there appear some differences within 0% and 24.5%. The latest seems to be an important one taking into account that we deal with small amounts of pharmaceutical substances. These differences could explain why after 1 hour from drug administration, the predicted ECBZ concentration in central compartment is with 25% higher than the observed one when we employed the numerical solution in comparison with 14% deviation when the analytical solutions were used. In this sense, every little difference in drug amount becomes significant and forces us to use the most precise method, which provides the pharmacokinetics parameters. Because the analytical solution is the gold standard in this field, and it does not propagate errors as numerical solution does, the first will be chosen in the process of simulation and the most precise parameters will be those obtained through implementation of the analytical solutions.

### Conclusions

Using the proposed method one can obtain the analytical solution for complex kinetic models with reduced dimensions directly by inspecting the graphical representation of the model (if there are involved only first order reaction or could be reduced at these). The new graphical method is an alternative to the classical flow graph method which uses the Laplace transforms, because, for the last, the complexity of reaching the analytical solutions limits its use.

Analytical solutions provide calculation of kinetic parameters with more accuracy, which is indeed an advantage, in comparison with numerical solutions, which may cause important errors. Another disadvantage of using numerical solutions is the slower process for reaching the convergence. This may be important when we deal with a great amount of data, especially in population PK analysis.

*Acknowledgements: This work was supported by a PNII-IDEI project, code 457, contract 393/2007 financed by CNCISIS Romania*

### References

1. GEX-FABRY, M., BALANT, L.P., Clin. Pharmacokinetics, **19**, 1990, p. 241
2. MA, M. K., ZAMBONI, W. C., RADOMSKI, K. M., FURMAN, W. L., Clin. Cancer Res., **6**, 2000, p. 813
3. BOXENBAUM, H. G., RIEGELMAN, S., HELASHOFF, R. M., J. Pharmacokin Biopharm, **2**, 1974, p.123
4. DINC, E., BALEANU, D., Rev. Chim. (Bucharest), **58**, no. 8, 2007, p. 816
5. MARIA, G, Rev. Chim. (Bucharest), **55**, no. 8, 2004, p. 628
6. UDRISTE, C., Aplicatii de algebra, geometrie si ecuatii diferentiale, Ed. Didactica si Pedagogica, Bucuresti, 1993, p. 264
7. JUERGEN, P., Reaktionskinetische Auswertung Spektroskopischer Hessdaten, Braunschweig, 1995, p. 160
8. CONNORS, K. A., Chemical Kinetics: The study of reactions rate in solutions, Hardcover, 1998, p. 67
9. OGATA, K., Modern Control Engineering, Prentice Hall International, New Jersey, 1995
10. NICE, N. S., Control System Engineering, Addison-Westley Publishing Company, 1995, p. 240
11. DORF, R. C., BISHOP, R. H., Modern Control System, Prentice Hall International, New Jersey, 2001, p. 66, 118
12. CRISTEA, M. V., AGACHI, S. P., Elemente de teoria sistemelor, Risoprint, Cluj-Napoca, 2002, p. 113
13. COMNAC, V., TOLLET, I., LAHTI, S., System Theory, Lux Libris, Braşov, 2004, p. 23
14. DIUDEA, M. V., GUTMAN, I., JANTSCHI, L., Molecular Topology, Nova, New York, 2002
15. IONESCU, T., Grafuri. Aplicatii, Ed. Didactică și Pedagogică, Bucureşti, **1**, 1973, p. 198
16. SOCOL, M., BĂLDEA, I., J. of the Chin. Chem. Soc., **53**, 2006, p.773
17. AITKEN, A. C., Determinants and Matrices, Oliver and Boyd, Edinburgh, 1939, Chap. 2
18. SOCOL, M., VLASE, L., Rev. Roum. Chim., **53**, no. 4, 2008, p. 297
19. SOCOL, M., BĂLDEA, I., J. Math. Chem., **45**, 2009, p. 478
20. LEMOS, O. A., VINCENZI, A. M., MALDONADO, J. C., MASIERO, P. C., J. of Systems and Software, **80**, 2007, p. 862

Manuscript received: 19.05.2005